Full Mesh Channel Measurements on Body Area Networks under Walking Scenarios

Matthieu Lauzier, Paul Ferrand, Antoine Fraboulet, Hervé Parvery and Jean-Marie Gorce
Université de Lyon, INRIA
INSA-Lyon, CITI-INRIA, F-69621, Villeurbanne, France
Email : matthieu.lauzier@insa-lyon.fr

***Abstract*—Body Area Networks (BANs) exhibit a unique form of channel variations and traditional propagation models fail to adequately match the behavior of BAN communication links. We present here the results of a measurement campaign whose primary objective was to characterize the complete mesh of a BAN and simultaneous analyze the quality of every radio link between the different nodes. We performed several measurement campaigns with indoor and outdoor walking scenarios. The data harvested allows us to highlight symmetry issues in the communications, and we prove that it is due in part to hardware variations in the sensors. Furthermore, the simultaneous measurements of the link quality allows us to extract the correlation in their temporal evolution. We show that scenario-based link correlation matrices cannot be considered, but their evolution over time is stable enough to consider that practical protocols may estimate them with sufficient precision.**

I. Introduction

Body Area Networks are a promising application in wireless sensors networks, both in the consumer area due to a large increase of connected appliances worn near one's body, and in more specialized fields like sports and medical care. Capitalizing on the existing infrastructure and on-body and in-body sensors, BANs have the ability to be of great help to professionals of these fields. Following this trend, IEEE launched the 802.15.6 to focus on BAN standardization, from channel modeling to the MAC layer. Many contributions for channel modeling have been proposed from various entities around the world, and the working document of the 802.15.6 task group on channel model summarizes the current status of the work (see [1] and references therein).

A large part of the contributions on BANs focus on wide-band communications, but the current radio commodity hardware is still centered on narrow-band technologies. Narrow-band channel sounding and modeling for BANs thus have a great value in nowadays applications, especially for the development of medium access layer protocols. All the existing models agree on the fact that the body generates a strong shadowing effect on the received signal, on top of the usual small-scale fading. The temporal evolution of the link's quality in BANs is also heavily dependent on the scenario considered, as a running subject will not exhibit the same variations as a sleeping one. The approach in the IEEE working group is centered on a decoupling of these effects, where the shadowing follows a Gaussian distribution whose parameters depend on the scenario considered. While this model lends itself well to statistical manipulation, it does not truly capture the specificity of BAN links.

In [2], the authors identified a strong correlation between the time-variations of several links, due to the fact that body movements have strong symmetrical and periodical properties. Measurement campaign by Takada and Kim [3], D'Errico and Ouvry [4] tend to strengthen this result. Measurements of simultaneous transmission is thus of great interest for BANs while the subjects are moving in a natural manner. This is a limitation for the usual network emitters and analyzers used in channel sounding, since they limit the movement and freedom of the subject, and studies are thus usually deferred to propagation simulators as in [5], [6].

Meanwhile, studies [4], [7] have shown that the fading and shadowing component of BANs vary slowly, which opens the possibility of doing channel measurements using real sensors nodes. Using a small number of nodes, previous works extracted data from star topologies [8], [9], but these campaigns are restricted to one or two transmitter nodes.

The measurement campaign and analysis we conducted in this study consider a standard BAN under walking scenarios, where we evaluate and log the link quality of every link in the network quasi-simultaneously. The section II describes the platform we built for this experiment. Section III presents the results of an extensive nested-factorial experiment, focusing on link symmetry in BANs. We are able to expose strong deviations from complete symmetry due to manufacturing differences, which is stable enough to average and cancel in upper-layer protocols. Section IV aims at evaluating spatial correlations between the links. Using statistical tests on correlation matrices from the litterature, we show that the mean correlation matrix for repeated passages in the same environment differs greatly from the instantaneous correlation matrices. On the other hand, we also show these matrices do not vary significantly over time, opening up the possibility for applied protocols to estimate them reliably. In section V we draw conclusions on this study and define perspectives for future works.

II. Experimental setup

A. Body Equipment

For the experiment we defined a BAN composed of 6 nodes, whose positioning is shown on Fig.1, following usual standard BAN setups. THe HiKoB FOX sensors [10] we used

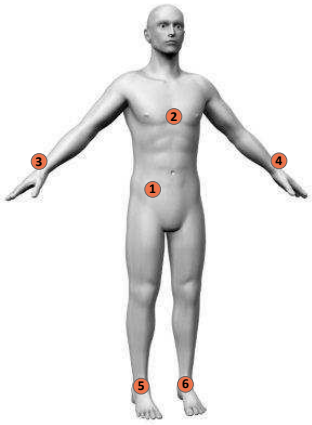

Fig. 1: Node positions on the body during the measurement.

embed a 32bits ARM Cortex M3 processor and an Atmel AT86RF231 radio chipset [11], for which the physical layer is IEEE 802.15.4 compliant in the 2.4GHz ISM band. They are particularly well suited for BAN measurements as they run on batteries, and are equipped with a μ-SD storage facility. These features allow us to deploy the measurement platform in any mobile indoor/outdoor scenario, and may store several hours of continuous data before saturating or powering down. The radio chipset used on the FOX sensor gives access to an Energy Detection (ED) metric, which is an average of the instantaneous Received Signal Strength Indication (RSSI) over the last 8 modulation symbols received. This metric offers a 1 dB relative error over the -91 dBm to -8 dBm range, [11] offering advanced analysis of its precision. In all the experiments the transmission power will be set to the maximum (3 dBm), to exploit the wider ED measurement range. Table I summarizes the important radio features of the FOX sensors, and specifically the high tolerance on the transmission power, which is a non-negligible factor for the link symmetry.

Modulation	Offset-QPSK with spreading
Frequency range	2408-2480 MHz
Inter-channel space	5 MHz
Max. transmission power	3 dBm (2 mW) $\pm$ **3 dBm**
Sensitivity	-101 dBm at 250 kbps
Antenna	Chip (integrated on the PCB)
Polarisation and gain	Omnidirectional (1 dBi)
Noise figure	6 dB

TABLE I: Main radio features of the FOX sensors.

B. Protocol design

As the coherence time in a BAN was measured around 125 ms for walking scenarios [4], we were able to design our protocol as a Time Division Multiple Access (TDMA), as illustrated in Fig.2, each node transmitting periodically in a pre-determined timeslot. The protocol we designed is auto-adaptive, which means it can adapt its period to any number of nodes. Each period can be divided into 8 slots: the first 6 slots are reserved for the transmission of each node (tipically its identifier, current frame number and additional control data), after what one transmission slot is reserved for a control node, which is used to start and stop the logging on the μ-SD card. When they are not transmitting, all the nodes are listening and collecting the data transmitted by the other nodes Finally, a longer timeslot is dedicated for logging onto the SD card all the information the nodes collected during a whole period. In order to assess the channel quality, the nodes store the ED measurement for each packet received. They also update their synchronization counter at each successful reception. The whole period duration (transmission + SD logging) is 12 ms, which according to [4] is sufficient to accurately evaluate the shadowing, mostly due to the body movement, on each link.

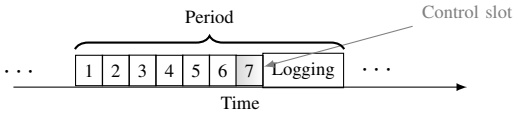

Fig. 2: Protocol used for the measurement campaign

III. Link symmetry

The protocol we use allows us to measure the direct and reverse path in a quasi-simultaneous manner. We are thus able to assert the validity of the symmetry hypothesis, commonly supposed in both protocol design and theoretical performance evaluation in wireless networks. The studied variable is the difference in received power by nodes in both directions on a link. Preliminary measurements and data-sheets for sensor hardware allowed us to identify two possible factors affecting the link symmetry:

- The different links are an inherent model factor, but as seen on Fig.3 links that have a lower average link quality seem more subject to asymmetry than high quality links. In particular, links with a weaker line-of-sight contribution will be more subject to multi-path fading effects, which can affect the link quality in a rapid and non-negligible manner.
- The data-sheet for the AT86RF231 radio [11] specifies that the transmission power is defined with a $\pm$ 3 dBm range relative to the value set at the beginning at the transmission, which could strongly affect the perceived link quality. The metric used in the measurement is also specified with a $\pm$ 1 dB relative error. This *sensor* effect may also include minute variations in the hardware, leading to varying noise figures and overall sensitivity to channel variations.

In order to evaluate the relative significance of these effects, we designed a cross factorial experiment as follows. We consider the upper-body links, namely positions 1 to 4 on Fig.1 indexed as $\{\mathrm{Hip}, \mathrm{Torso}, \mathrm{RightHand}, \mathrm{LeftHand}\}$, and 4 sensors indexed $\{1, \ldots, 4\}$. We rotated each node on the body positions and we walked along the same exact path 3 times in a

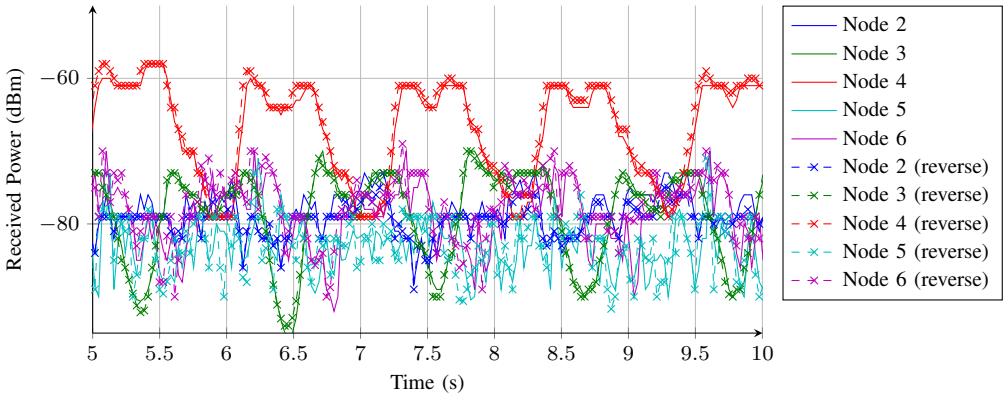

Fig. 3: Zoom on the link quality measured by node 1 (Hip) during an outdoor walking experiment.

row, effectively incorporating a *passage* effect into our model. This effect is hierarchical ; for each link and sensor position, we have 3 passages. In contrast with the other effects, the passages are *random* in the sense that they do not represent a level of the factor, but are rather drawn from all possible passages each time [12]. We thus have 6 different links and couple of sensors, which translate into 6 levels for each factor. This experiment was conducted outdoor, in a running track on our campus, far for interfering equipments.

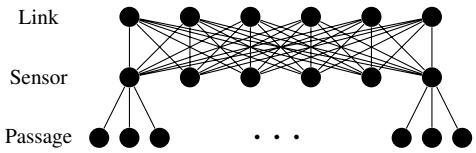

Fig. 4: Schematic representation of experiment.

Our experiment form is termed *nested factorial*, composed of two fixed effects – the links and sensor couples – and a random passage effet. The significance of each identified effects may be studied using Analysis of Variance (ANOVA) techniques, as described in [12, Ch.6-7]. The result of the ANOVA is represented in Tab.II, where we give the various sum of squares (SS), mean squares (MS) and degrees of freedom of each effect and their interaction. The F and p values represent the associated F statistic and the significance level of the factor.

From the table II, it is clear that the passages have no significant effect at a 5% significance level, as indicated by a p-value of 0.09. On the other hand, both the links and sensor have a strong effect on the link symmetry, as does their interaction. The relative mean divergence of each effect is seen on Fig.5 where we plot the mean deviations of each sensor couple for the links in our network. We can visually form several group from the figure ; first and foremost, the behavior of sensor couples $(1-3)$ and $(1-4)$ is very similar, as is the behavior of couples $(2-3)$ and $(2-4)$ but with more interactions. The couple $(1-2)$ has a behavior which looks similar to $(1-3)$ without being completely unaffected by the interactions ; likewise, couple $(3-4)$ shows a fair resemblance with $(2-3)$ and $(2-4)$. Between those two apparent groups, the interaction effect is thus significant, as indicated by Tab.II, but within the groups the effect that predominates any other is clearly the sensor effect rather than the link effect. The case of couple $(1-2)$ is especially representative of the deviation, averaging a whole 1.5 dB above the mean, whereas the other couples stay in the $\pm$ 1 dB range.

Although these variations seem important at first sight, we have to consider that both the link and sensor effect are not varying factors in real sensor networks. While we have to assess the validity of the relative insignificance of repeat passages, real protocols may compensate over time for the mean deviation of the links and sensors through standard averaging. This opportunity nevertheless requires symmetric

Effect	SS	d.f.	MS	F	p
Link	4515	5	902.81	590.34	0
Sensor	166244.9	5	33248.98	21740.29	0
Link × Sensor	11836.3	25	473.45	57.96	0
Passage(L,S)	1120.3	72	15.56	1.37	0.09
Error	732596.7	479409	1.53		
Total	920779.2	479516			

TABLE II: ANOVA table for the experimental results.

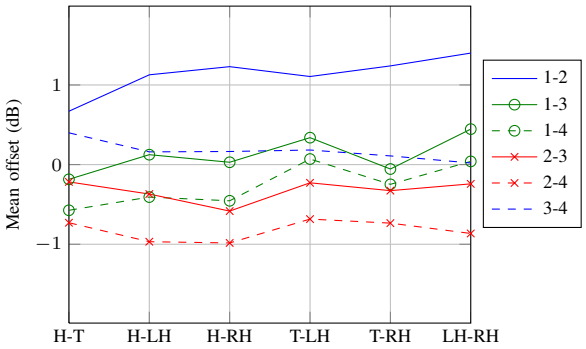

Fig. 5: Interactions between the sensor effect and the link effect for the experiment of Sec.III.

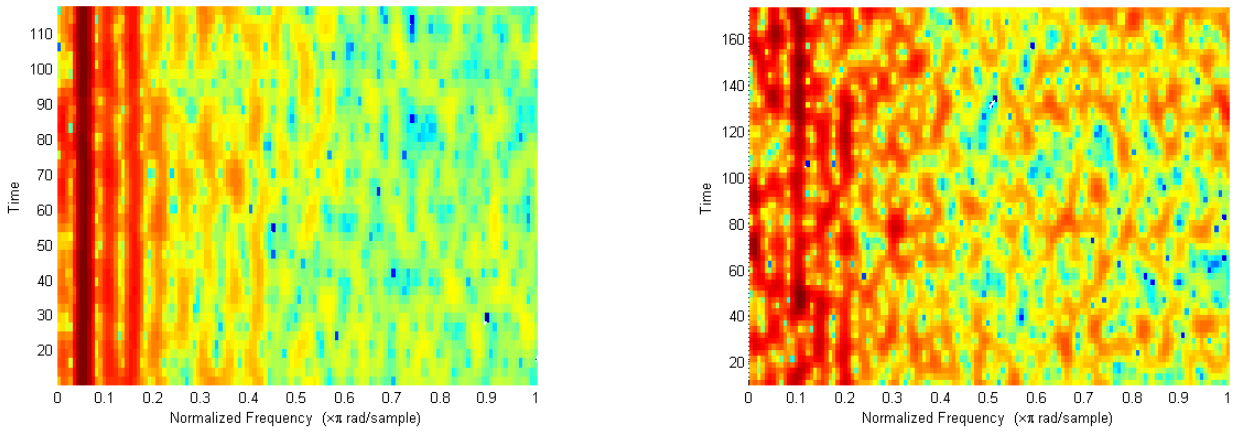

(a) Outdoor

(b) Indoor

Fig. 6: Spectrograms of a passage in each scenario, for the Left Hand → Hip link.

measurements of the link quality by the nodes in the network, which is rarely included in common protocols.

IV. Shadowing correlation

For the second measurement campaign, we chose locations with a low amount of interference both indoor and outdoor. The outdoor scenario was conducted on the same running track as Sec.III, and the indoor scenario was conducted in a corridor located in a basement, which is interference-free and narrow, thus highly prone to multipath reflections. The measurements consisted in 10 passages over the same path.

A preliminary work focused on the separation between the fast fading effects and the shadowing due to the movement. As seen on Fig.3, the body movements generate strong periodical variations in the link qualities. The analysis of their spectrograms for the outdoor scenario shows that outdoors these variations generate low frequency components (Fig.6a), the fundamental peak being centered around the movement frequency. On the other hand, for the indoor scenario, the spectrum tends to spread towards a uniform pattern, which means the influence of the shadowing due to the body motion is much less significant ; this can be explained by a relatively more important contribution of the multipath reflections in the received power. In this case we wouldn't be able to properly extract the shadowing effects, and a fading-only model may in fact be better suited for the channel. Concentrating on the outdoor scenario, we eliminated the fading components with a Butterworth low-pass filter, for which we defined the cutoff frequency at about 3 Hz. This performs a satisfactory extraction of the three major shadowing components.

The objective of our work is to analyze the spatial correlations of the shadowing effects, and specifically their stability, at several levels. The tests of Jenrich [13] and Larntz [14] on the equality of correlation matrices are particularly well-suited for this purpose, although an in-depth description is out of the scope of this paper. Following the standard hypothesis testing framework, the equality is evaluated with respect to a significance level α. This significance level, in this case, is equal to the probability of assuming that the matrices are equal when they are not – a false positive. Both tests are asymptotically correct, and have satisfying statistical powers, although as shown in [14], Jennrich's test loses power on small populations.

We first compute the global mean correlation matrix over all the passages, and to test the correlation matrix of each individual passage against it. *In every case, both tests concluded with very high significances ($\alpha < 0.01$) that the individual correlation matrices of the passages are not equal to the mean one.* The impact of this result is very important, as we have to conclude that it is no meaningful to consider a global correlation matrix for the modelisation of a specific BAN scenario.

Step	1	2	3	4	5
Passage 1	2.20	1.84	2.96	2.79	1.80
Passage 2	3.80	3.12	2.63	2.67	2.43
Passage 3	1.74	2.17	1.98	1.35	2.04
Passage 4	2.81	2.12	2.56	3.25	2.86
Passage 5	2.51	3.31	2.96	2.58	3.90
Passage 6	2.47	2.07	3.11	2.68	2.52
Passage 7	2.05	1.77	2.32	2.19	1.80
Passage 8	1.92	2.42	1.56	1.81	1.92
Passage 9	2.60	1.31	3.47	3.11	2.37
Passage 10	1.99	2.48	3.80	2.60	1.99

TABLE III: Larntz' statistic value of equality for the correlation matrices computed at each step w.r.t. the next step, excluding the node located on the torso. Dark red cells represent significance at $\alpha = 1\%$, light red at $\alpha = 5\%$.

We then focused on the behavior of the correlation matrices on a shorter time-scale, evaluating the equality between the consecutive correlation matrices at each step for each passage. Since we base the correlation matrix estimations on a reduced amount of samples, we only use Larntz's statistical test. In this case, we obtained significant differences between the correlation matrices, but another test performed without the

node located on the torso yielded much more stable results, as shown in Table III, where 5 steps are considered per passage. It is thus possible, for this group, to estimate the correlation matrix for the next step from the correlation matrix of the current step. We finally compared the correlation matrices computed at each step, with the global correlation matrix computed for each passage. These results, presented in Table IV for the 5 first steps of each passage, also show that for each passage we obtain rather stable values, thus the assertion of the correlation stability could be valid on a longer time-scale, although these results exhibits some differences from one passage to another.

Step	1	2	3	4	5
Passage 1	3.88	3.25	2.89	2.18	3.25
Passage 2	4.57	3.20	3.38	3.89	2.38
Passage 3	2.70	1.66	2.90	2.88	1.76
Passage 4	2.80	1.92	2.58	3.49	3.83
Passage 5	2.97	3.31	2.04	2.14	4.83
Passage 6	3.08	2.56	2.38	1.91	3.71
Passage 7	1.75	2.05	2.40	2.32	2.26
Passage 8	1.99	2.75	1.73	2.37	2.64
Passage 9	2.25	3.20	2.50	2.57	1.38
Passage 10	3.57	2.12	3.64	2.50	2.20

TABLE IV: Larntz' statistic value of equality for the correlation matrices computed at each step with the correlation matrix of each passage, excluding the node located on the torso. Dark red cells represent significance at $\alpha = 1\%$, light red at $\alpha = 5\%$.

V. Conclusion and perspectives

The design of a platform dedicated to the study of BAN channels using industrial sensors, allowed us to conduct an important measurement campaign based on walking scenarios. The use of industrial sensors, in spite of a lower precision on the measurement of link quality, offer more freedom in the choice of the scenario than the usual channel sounding equipment, a total mobility and a high storage capacity.

The different works conducted on the collected data tend to emphasize the following points:

- The radio chipset embedded on the sensors have a high transmission power tolerance and the *Energy Detection* presents a lack of accuracy, but in spite of these imprecisions we can still extract significant results on BAN channels.
- An important asymmetry could be observed, especially on the links with important fading. The impact of the passages on the symmetry of the links is negligible compared the sensor hardware and the link influences.
- The application of a low-pass filter on the frequency analysis of the links allowed us to extract the shadowing effect caused by the body motion, on the outdoor scenario, for which this effect is obviously dominant in the low frequencies. For the indoor scenario, as the links are more prone to multipath fading, the shadowing effect does not clearly appear and thus cannot be extracted reliably.
- The differences between the shadowing correlation matrices is significant from one passage to another, and as such it may not be meaningful to consider a global correlation matrix for a given BAN scenario.
- The correlation matrices present short-term and medium-term similarities, if we consider a selected group of nodes. Assuming the correlation matrix at time $t+1$ is close to the correlation matrix at time t is thus statistically valide, and would be of great interest in realistic protocols for the elaboration of relaying strategies.

The first perspective of this work would be to extend the scenarios considered. This will lead to the building of an important database, which will be useful for further analyses. We also conducted preliminary work on network simulators to "replay" the measurements and thus act as realistic BAN simulators for the development and testing of communication protocols. An important improvement would be the design and integration on the sensors of a daughterboard dedicated to channel measurements, as done in [2], in order to increase the measurement accuracy. Long-term simultaneous link measruement also opens the possibility of advanced channel modeling. We plan, for example, to use these measurements to fit existing models in the litterature capturing the temporal evolution of the BAN links, are illustrated in [2], [4] with time series, and in [7] with Markov models.

References

[1] K. Yazdandoost and K. Sayrafian Pour, "Channel Model for Body Area Network (BAN)," http://math.nist.gov/mcsd/savg/papers/15-08-0780-09-0006-tg6-channel-model.pdf, 2009.

[2] S. Cotton, G. Conway, and W. Scanlon, "A Time-Domain Approach to the Analysis and Modeling of On-Body Propagation Characteristics Using Synchronized Measurements at 2.45 GHz," *Antennas and Propagation, IEEE Transactions on*, vol. 57, no. 4, pp. 943–955, 2009.

[3] Minseok Kim and J.-I. Takada, "Statistical Model for 4.5-GHz Narrowband On-Body Propagation Channel With Specific Actions," *Antennas and Wireless Propagation Letters, IEEE*, vol. 8, pp. 1250 –1254, 2009.

[4] R. D'Errico and L. Ouvry, "A Statistical Model for On-Body Dynamic Channels," *International journal of wireless information networks*, vol. 17, no. 3-4, pp. 92–104, 2010.

[5] M. Gallo, P. S. Hall, Qiang Bai, Y. I. Nechayev, C. C. Constantinou, and M. Bozzetti, "Simulation and Measurement of Dynamic On-Body Communication Channels," *IEEE Transactions on Antennas and Propagation*, vol. 59, no. 2, pp. 623–630, 2011.

[6] P. Ferrand, M. Maman, C. Goursaud, J.-M. Gorce, and L. Ouvry, "Performance evaluation of direct and cooperative transmissions in body area networks," *Annals of Telecommunications*, pp. 1–16, 2011.

[7] Jian Zhang, D. B. Smith, L. W. Hanlen, D. Miniutti, D. Rodda, and B. Gilbert, "Stability of Narrowband Dynamic Body Area Channel," *IEEE Antennas and Wireless Propagation Letters*, vol. 8, pp. 53–56, 2009.

[8] V. G. Chaganti, D. B. Smith, and L. W. Hanlen, "Second-Order Statistics for Many-Link Body Area Networks," *IEEE Antennas and Wireless Propagation Letters*, vol. 9, pp. 322–325, 2010.

[9] Minseok Kim, K. Wangchuk, and J. Takada, "Link correlation property in WBAN at 2.4 GHz by multi-link channel measurement," in *Proc. 6th European Conf. Antennas and Propagation (EUCAP)*, 2012, pp. 548–552.

[10] "HiKoB FOX sensor," http://www.hikob.com/hikob-fox, 2012.

[11] "AT86RF231," http://www.atmel.com/devices/at86rf231.aspx, 2012.

[12] C. Hicks and K. Turner, *Fundamental Concepts in the Design of Experiments*, 5th ed. Oxford University Press, 1999.

[13] R. I. Jennrich, "An asymptotic χ^2 test for the equality of two correlation matrices," *Journal of the American Statistical Association*, vol. 65, pp. 904–912, 1970.

[14] K. Larntz and M. D. Perlman, "A simple test for the equality of correlation matrices," Department of Statistics, University of Washington, Tech. Rep., 1985.